ME-NETT23 The 23rd Conference of the Mechanical Engineering Network of Thailand

E-DRC-001464

The 23rd Conference of the Mechanical Engineering Network of Thailand
November 4 – 7, 2009, Chiang Mai

A Vibration Sensing Device with Differential Slotted Optical Switch for Active Vibration Isolation Applications

Wichaphon Fakkaew*, Theeraphong Wongratanaphisan,
Matthew O.T. Cole, Radom Pongvuthithum

[1]Chiang Mai University, 239 Huay Kaew Road, Muang, Chiangmai, 50200
*Corresponding Author: wichaphon_me@hotmail.com, Tel. 08-1716-9499

Abstract

This paper presents the design of a Vibration Sensing Device (VSD) based on a sprung-mass mechanism with a differential slotted optical switch sensor. The basic characteristics of an optical switch that obtained off-the shelf were studied through experiment. The working principle of a non-contact displacement sensor based on the differential slotted optical switch is presented. The displacement sensor is employed to observe the relative displacement of a proof mass in order to detect vibration in an active vibration isolation platform. A membrane spring is employed to support the proof mass. The sensitivity and bandwidth of this vibration sensing device is tested and reported. A discussion on compensating for nonlinear effects and the self-heating effect of the sensor is also provided.

Keywords*:* Vibration Sensor, Differential displacement sensor, Sensor design, Vibration Isolation, Slotted optical switch.

1. Introduction

Microvibration isolation has become a growing research field due to the demands of high-precision systems, and the advent of micro- and nano-technology in various scientific and industrial processes. Although conventional passive isolation mounts are widely used, they have an inherent trade-off between good high-frequency isolation and amplification of vibration near resonant frequencies. In principle, the best isolation performance is achieved by using an active system in combination with a passive mount, as low-frequency resonances can be actively controlled while preserving the high-frequency performance. In active systems, high sensitivity, high bandwidth sensors have been employed to avoid the need to consider sensor dynamics in the system model and controller design. However, the bandwidth of sensors is often much higher than the required isolation range and their cost is usually high. In principle, good performance is achievable even without high bandwidth sensors if sensor dynamics are considered in the controller design. This prompts

the notion of developing low cost sensors with high sensitivity but not necessarily high bandwidth.

In this paper, a displacement sensor with differential slotted optical switch is applied in the design and construction of a vibration sensing device (VSD).

2. Displacement sensing by slotted optical switch

A slotted optical switch consists of an infrared emitting diode and an NPN silicon phototransistor separated by a small gap. Such switches have many applications such as shaft encoders, noncontact limit switches etc. The design of a slotted optical switch is typified by the OPB804 from OPTEK Technology Inc., as shown in figure 1. The device can be used directly as a non-contact displacement sensor in conjunction with a shield object if the relation between shield displacement and output current has a wide enough linear range. The main characteristics of a slotted optical switch are discussed in the following subsections.

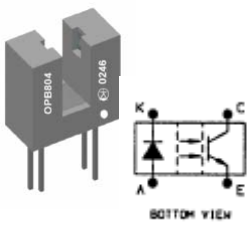

Fig. 1 Slotted optical switch OPB804

2.1 Characteristics of a slotted optical switch

Current-displacement characteristics of a typical single slot optical switch (OPB804) have been obtained using the test circuit shown in figure 2a. Figure 2b shows the relation between the normalized collector current at steady state I_r and the normalized shield displacement y_r. This relation has been identified using the standard S-curve function of the form:

$$\tilde{I} = \frac{1}{e^{\alpha y_r} + 1} \qquad (1)$$

where $\alpha = 28.93$, $\tilde{I} = i_s / I_{C(ON)}$ and $\tilde{y} = (y - y_{CL}) / 2y_{CL}$. The collector current at steady state, i_s, is obtained by $i_s = v_{os} / R$ where v_{os} is the output voltage at steady state. The ON-state collector current, $I_{C(ON)}$, was measured at 15.65 mA with V_D set at 10 V. y is shield distance and $y_{CL} = 1620\mu m$ is the shield distance at which the collector current is half of the ON-state collector current.

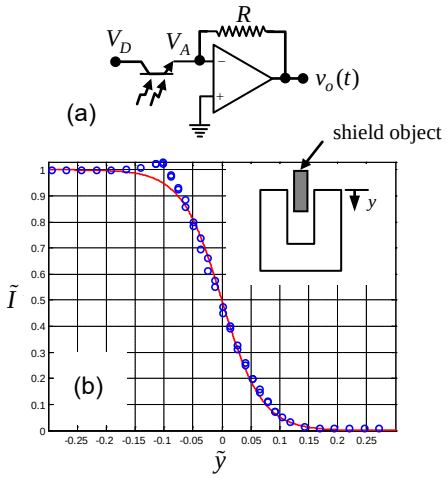

Fig. 2 Current-distance characteristic of a slotted optical switch OPB804, (a) test circuit (b) test results.

2.2 Design of a differential displacement sensor

A differential arrangement is frequently used in sensor design to improve linearity [1,2]. Consider the normalized collector current $\tilde{I}$ in terms of Taylor series expansion around the operating (normalized) shield displacement $\tilde{y}_0$:

$$\tilde{I}(\tilde{y}) = \tilde{I}(\tilde{y}_0 + \tilde{d}) = \tilde{I}(\tilde{y}_0) + \left.\frac{\partial \tilde{I}}{\partial \tilde{y}}\right|_{\tilde{y}_0} \tilde{d} + \frac{1}{2!}\left.\frac{\partial^2 \tilde{I}}{\partial \tilde{y}^2}\right|_{\tilde{y}_0} \tilde{d}^2 + \ldots \qquad (2)$$

The first term in (2) represents an offset current and the coefficient in the second term represents the device sensitivity. The remaining high order terms can be regarded as nonlinear effects and are usually neglected.

For the differential arrangement shown in figure 3a, the change in normalized collector current $\Delta\tilde{I}$ from the value at the nominal position is

$$\begin{aligned}\Delta\tilde{I} &= \tilde{I}(\tilde{y}_0 - \tilde{d}) - \tilde{I}(\tilde{y}_0 + \tilde{d}) \\ &= 2\frac{\partial\tilde{I}}{\partial\tilde{y}}\Big|_{\tilde{y}_0}\tilde{d} + \frac{2}{3!}\frac{\partial^3\tilde{I}}{\partial\tilde{y}^3}\Big|_{\tilde{y}_0}\tilde{d}^3 + \frac{2}{5!}\frac{\partial^5\tilde{I}}{\partial\tilde{y}^5}\Big|_{\tilde{y}_0}\tilde{d}^5 + \ldots\end{aligned} \quad (3)$$

Here, the offset and the dominant second-order nonlinear terms cancel. However, the nonlinear effects can be further reduced by setting $\tilde{y}_0 = \tilde{y}_c$ where $\partial^3\tilde{I}/\partial\tilde{y}^3\,|_{\tilde{y}_c} = 0$. For the case $\alpha = 28.93$ this requires $\tilde{y}_c = \pm 0.0454$. The sensitivity of differential normalized collector current $K_I = 2(\partial\tilde{I}/\partial\tilde{d})_{\tilde{y}_0}$ is plotted against normalized displacement of shield object $\tilde{d} = d/2y_{CL}$ in figure 3b.

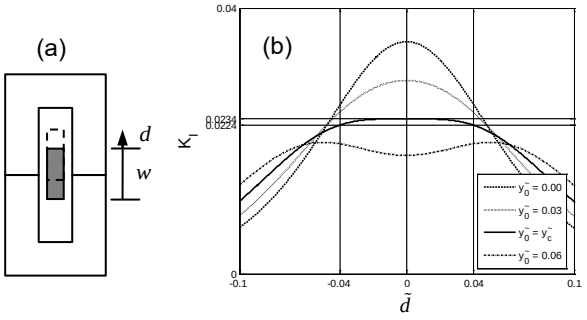

Fig. 3 The sensitivity of different normalized collector current at the various initial normalized shield distance

In figure 3b, when $\tilde{y}_0$ was set to be equal to $\tilde{y}_c$, the sensitivity curve was flat around the inertial setting and the linear range to with in $\pm 2\,\%$ was obtained between $-0.04 < \tilde{d} < 0.04$ or $-130\mu\text{m} < d < 130\,\mu\text{m}$, and the optimal width of the shield object was found to be $w/2 - y_{CL} = \tilde{y}_c \times 2y_{CL}$ or $w = 3.5\,\text{mm}$. The output current at steady state can be obtained by

$$i_s(d) = K_I \times d \quad (4)$$

where $K_I \approx 0.0229 I_{C(ON)}$ and $d \in (-130, 130)\mu\text{m}$.

2.3 Self-heating effect

When operating, the optical transistor is subject to a self-heating effect, which can create a lag component in step response and thus error over the low frequency range [3]. The effect is due to the power dissipation within the transistor when conducting. A self-heating effect model and self compensation approach can be found in [4]. Here we discuss the consequences of this effect on our vibration sensing device in the experimental section and demonstrate that it is not significant.

3. Design of vibration sensing device

There are many ways to measure the vibration of a solid platform. One way is to use a simple sprung proof mass mechanism where the vibration of the solid platform can be observed by the relative displacement of the sprung proof mass. Consequently, we can combine the sprung proof mass mechanism with the differential displacement sensor to construct a VSD. In this section, the design considerations for the VSD will be presented.

The schematic diagram of a VSD considered in this study is shown in figure 4a and the construction of the VSD is shown in figure 4b. The VSD consists of a proof mass supported by two membrane springs holding a shield, which moves in the slots of an optical switch pair. The design prevents lateral motion so that contact between the shield and the side of the slot is avoided. The pair of slotted optical switches operates as a differential displacement sensor

which detects the relative displacement of the proof mass and the shield.

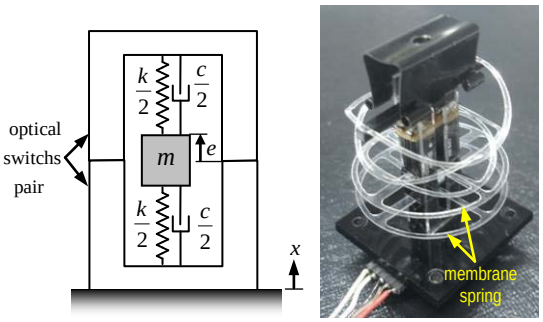

(a) (b)

Fig. 4 (a) The schematic diagram of the VSD and (b) the construction of VSD

The relation between the relative displacement e of the proof mass, m, and sensor body displacement, x, of the VSD is given by

$$\ddot{e} + \frac{c}{m}\dot{e} + \frac{k}{m}e = -\ddot{x} \qquad (5)$$

where k and c are the stiffness of the spring support and the damping coefficient respectively as shown in figure 4(a). The characteristic of the VSD can be specified by selecting the stiffness of the membrane spring. In addition, the damping coefficient is associated with the material damping of the membrane spring, therefore, it is an unadjustable parameter.

In our study, two VSDs with different stiffnesses were made. The lower stiffness device will be referred to as *Sensor1* and the higher stiffness device as *Sensor2*.

4. Experimental results and discussion

The characteristics of the VSD including sensitivity, transverse sensitivity, signal to noise ratio and drift were tested and the experimental results are as follows.

The sensitivity of the VSDs was obtained by frequency response measurement. The VSDs were placed on shaker table, for which the amplitude and frequency of vibration could be varied and its acceleration could be observed by a seismic accelerometer. The experimental results are shown in figure 5. The results match well with the simple model (eq. 5) in the range of tested frequencies. The natural frequency and damping ratio of each sensor was identified as shown in table 1.

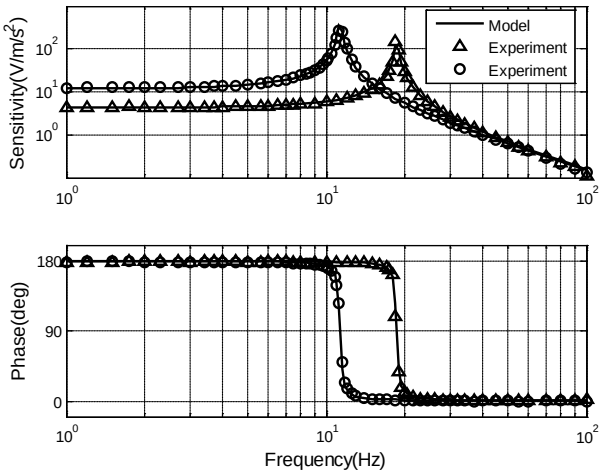

Fig 5. Frequency response of VSDs

Table 1 Parameter of VSDs obtained from the identifications.

Sensor	m (g)	f_n (Hz)	ζ	k (N/m)	c (Ns/m)
1	1	11.2	0.015	4.95	0.0037
2	1	17.8	0.015	12.5	0.0094

Some characteristics of the VSDs are dependent on the natural frequency and damping ratio. If the vibration sensing device is to be used as an accelerometer, the standard operating frequency range is in the zone where the frequency response graph is flat. In this zone, the sensitivity of the VSD is independent of the frequency, so that the output voltage is only dependent of the acceleration magnitude. Therefore, higher natural frequency gives wider

operating frequency range but lower sensitivity. Although the natural frequency can be increased by using stiffer membrane spring, this reduces the sensitivity of the device so that signal to noise ratios resulting form the sensor and conditioning circuit would worsen over the low frequency range where good performance is necessary for control purposes.

The frequency response test results indicate that the self-heating effect is negligible for the frequency range considered as the magnitudes and phase match well with the seismic accelerometer even for low frequencies, where the self-heating effect has most influence.

Transverse sensitivity of a sensor refers to the output caused by motion at 90 degrees to the measurement axis. Ideally this should be as small as possible. Generally, it is expressed as a percentage of the axial sensitivity. In order to test the transverse sensitivity, the VSDs were placed with the measurement axis in the vertical direction onto a shaker table that moves in the horizontal direction.

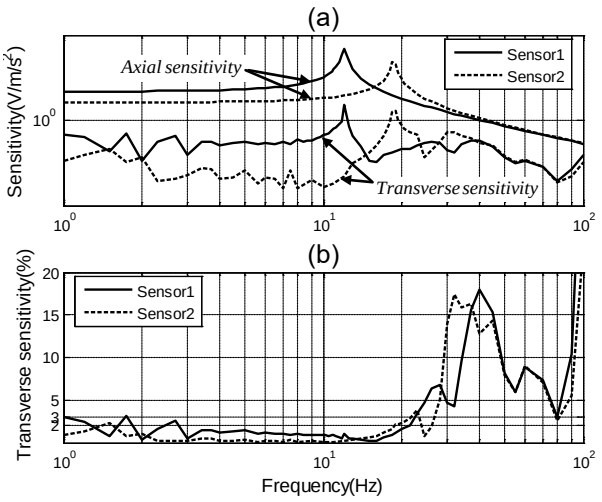

Fig 6. Transverse sensitivity of VSDs

The frequency response in the transverse direction compared with axial direction is shown in figure 6a and the transvere sensitivity in terms of the percentage of axial sensitivity is shown in figure 6b. The transverse sensitivity is quit high in the high frequency range (20 – 100 Hz) which indicates the strong coupling between transverse and axial directions. If this VSD is applied in a process that involves multidirectional vibration in multi-direction e.g. multi-axis vibration isolation system, the high frequency signal from the VSD will not be reliable for direct measurments of acceleration. However, the transverse sensitivity is less than 3 % in the frequency range between 1 – 20 Hz.

The signal-to-noise ratio for the vibration sensing device was found to be quite reasonable. Figure 7 shows the signal of the vibration sensing device compared with a seismic accelerometer. Both are used to measure the sinusoidal motion of a solid surface. Although, noise levels of the vibration sensing device are higher than the seismic accelerometer, the sensitivity of the vibration sensing device is higher. Therefore, it is clear that in term of signal to noise ratio, the vibration sensing device and the seismic accelerometer are comparable in low frequency range.

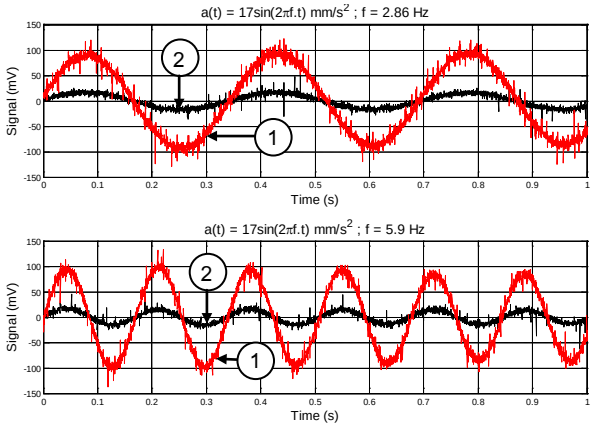

Fig 7. Output signal from the Sensor 2 (1) compare with a seismic accelerometer (2)

Drift is defined as slow changes in the output signal independent of the measured property. Figure 8 shows the output signal of the VSD with no excitation. Drift levels of the VSD are significant. By monitoring the output from each slotted switch separately we found that the same drift was observed in each output (figure 8). It can therefore be concluded that the output drift is caused by actual motion of the sprung proof mass system rather than electrical effects in the sensor circuits. However, the mechanism that causes drift of the sprung proof mass system is not yet fully understood, although it is likely to be an uncontrolled environmental disturbance.

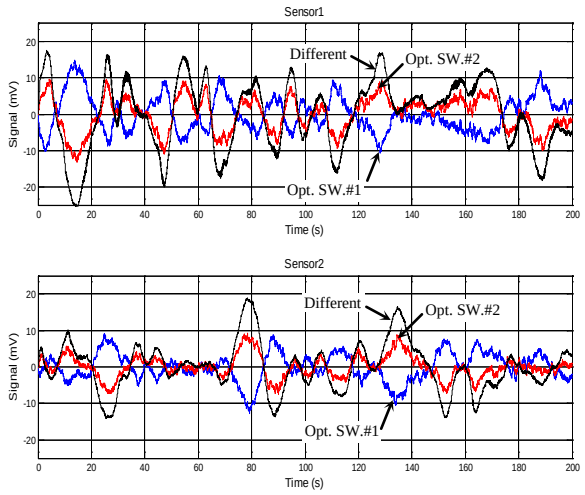

Fig 8. Sensor drift

There are two ways to overcome the sensor drift problem when the VSDs are included in an active vibration isolation system. One way is to use a high pass filter for signal conditioning, the dynamics of which must then be including in the sensor model for controller design. The other is to design a controller that is sufficiently insensitive to these very low frequency signals but still provides adequate control action (isolation) at higher frequencies.

5. Conclusion

Vibration sensing devices based on a sprung-mass mechanism and differential slotted optical switch have been designed, constructed and tested. Design criteria that can extend the linear range of the differential displacement sensor have been presented. Signal-to-noise ratios of the VSD prototypes were found to be quite satisfactory but very low frequency signal drift was significant. Overcoming this problem can lead to achieving the goal of a low cost sensor for an active vibration isolation system. In future work, the VSDs will be included and tested in operation on a multi-axis active vibration isolation platform.

6. Acknowledgement

This work was funded by the Thailand Research Fund through the Royal Golden Jubilee Ph.D. Program (Grant No. PHD/0227/2550) and NECTEC (Grant No. NT-B-22-E5-11-49-09).

7. References

[1] Topolnicki, J. and Skoczylas, N. (2007). Low cost dislocation sensor with differential capacitor *Sensors and Actuators A: Physical*, vol.140(2), November 2007, pp. 139-144

[2] Zhao, C., Wang, L. and Kazmierski, T. (2007) An efficient and accurate MEMS accelerometer model with sense finger dynamics for applications in mixed-technology control loops, paper presented in *IEEE Behavioral Modeling and Simulation Conference (BMAS 2007)*, California, USA

[3] Sinha, K.R.; Carter, R.L.; Russell, H.T. and Davis, W.A. (2008) Impact of Self-Heating on Frequency Response of Current Mirrors in Bipolar Technology, paper presented in *IEEE Region 5 Conference 2008*, Missouri, USA

[4] Yu Zhu; Twynam, J.K.; Yagura, M.; Hasegawa, M.; Hasegawa, T.; Eguchi, Y.; Amano, Y.; Suematsu, E.; Sakuno, K.; Matsumoto, N.; Sato, H.; and Hashizume, N.; Self-Heating Effect Compensation in HBTs and Its Analysis and Simulation, *IEEE Transactions on Electron Devices,* vol48(11), November 2001 pp. 2640 – 2646